Supplementary Figure 1

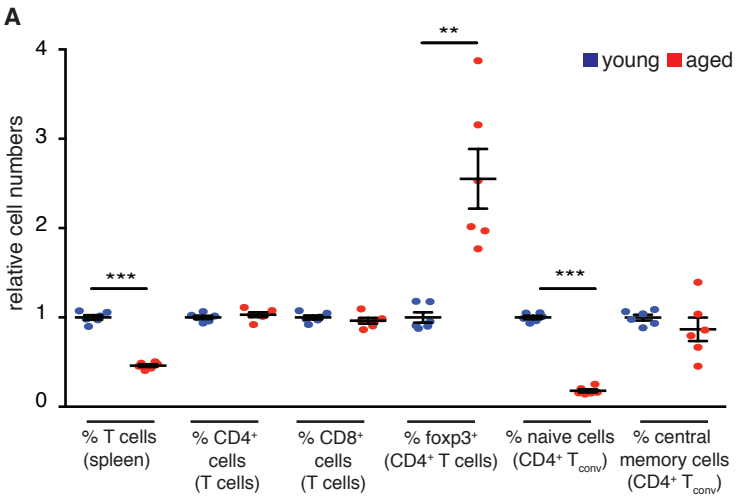

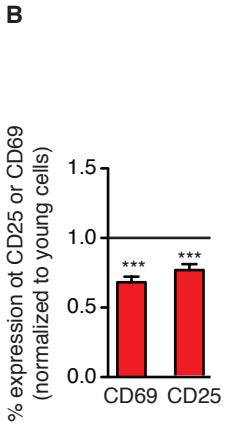

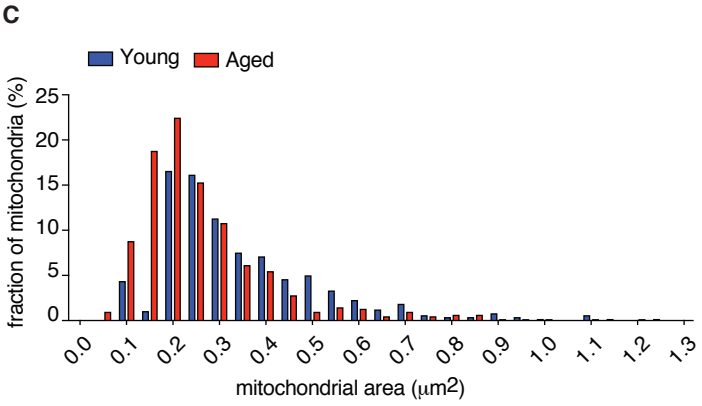

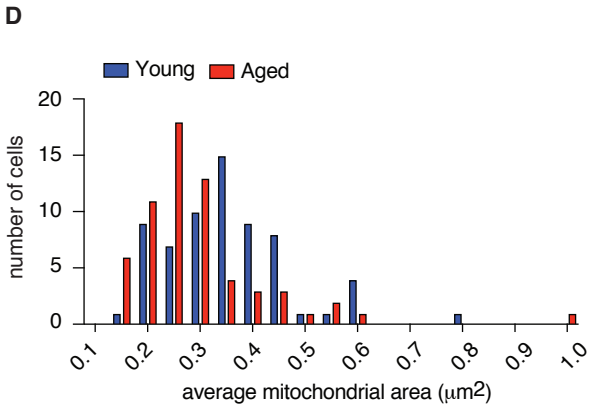

Supplementary Figure 2

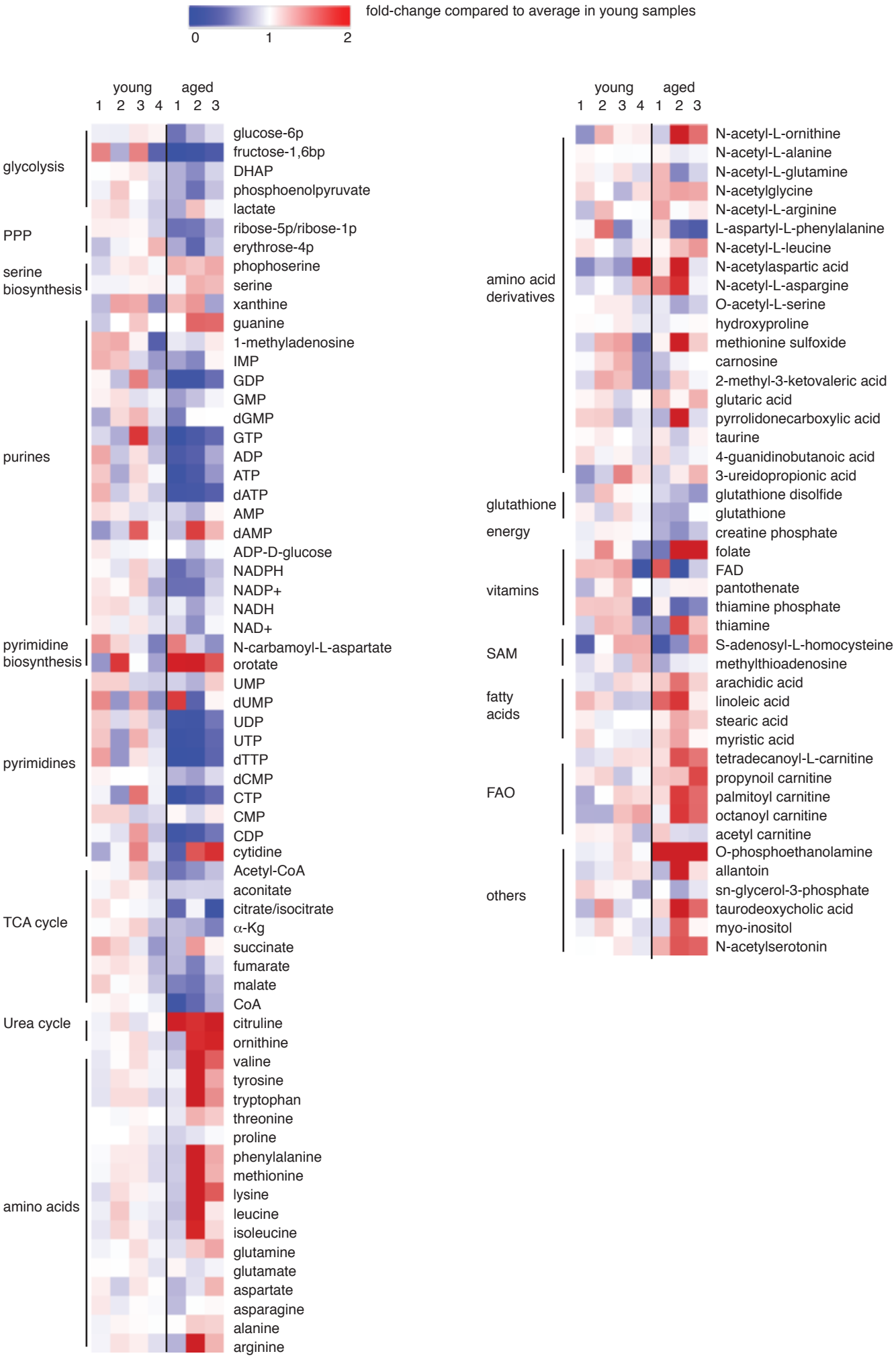

Supplementary Figure 3

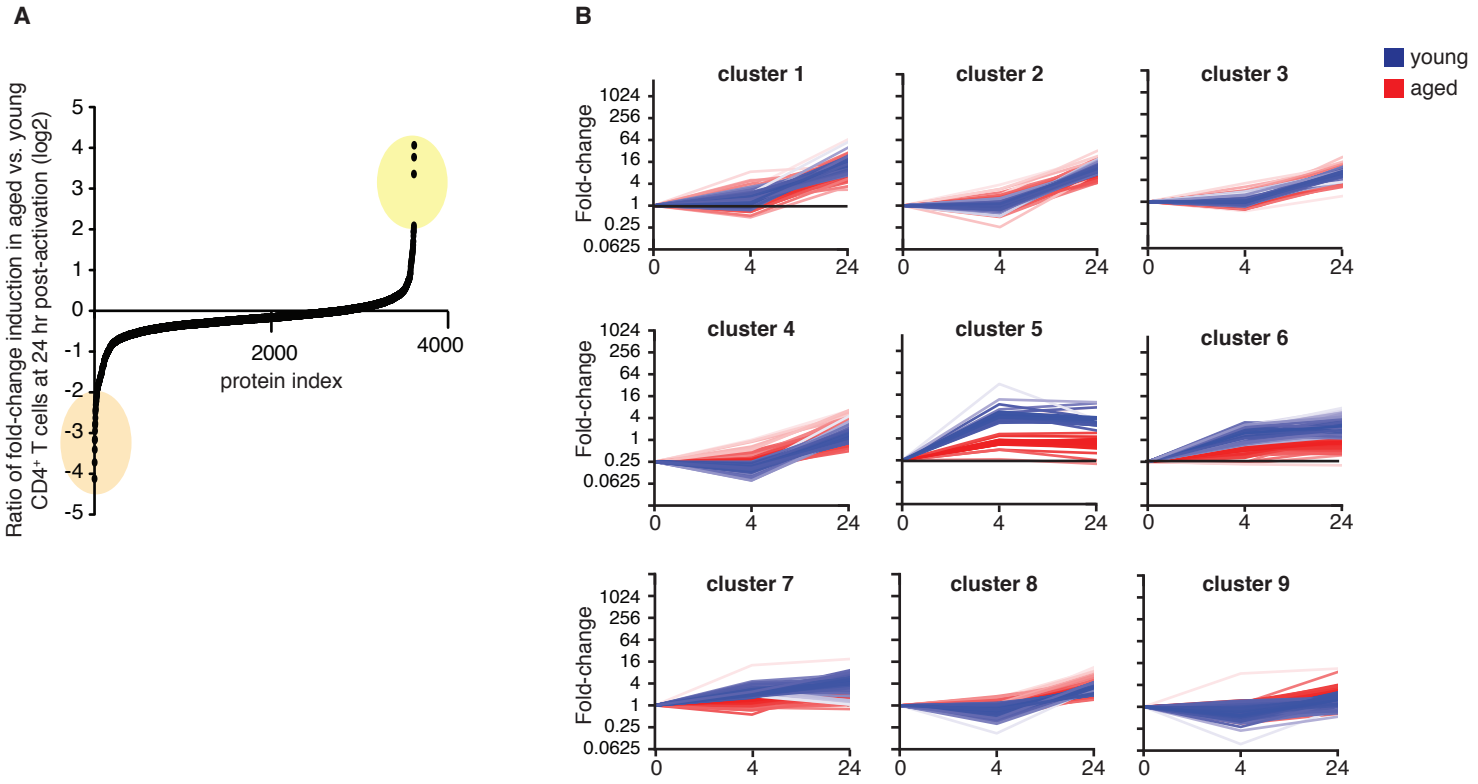

Supplementary Figure 4

A

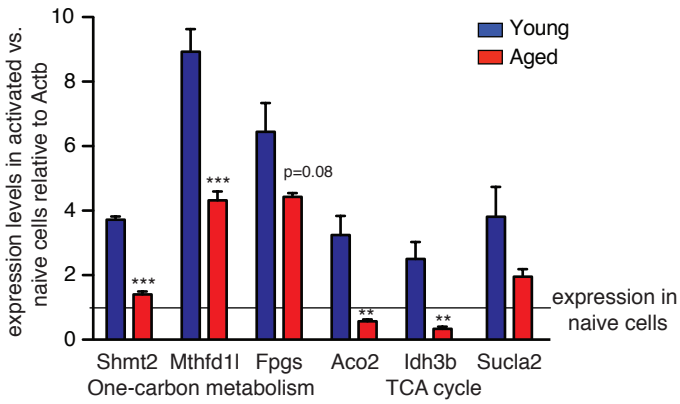

Supplementary Figure 5

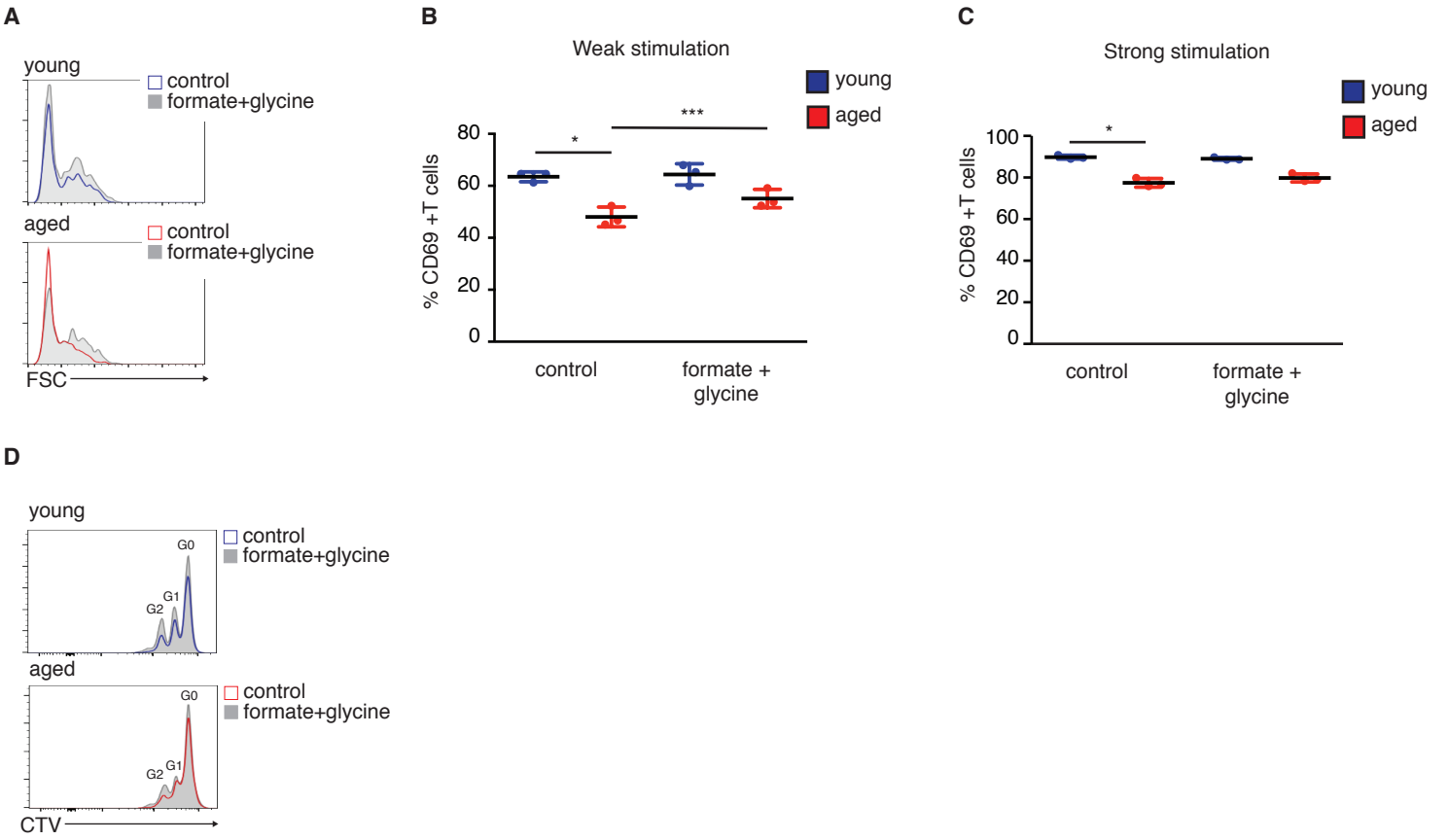

Table S1: The most differentially induced mitochondrial proteins in aged vs. young T cells

Proteins induced less in aged vs. young T cells			Proteins induced more in aged vs. young T cells		
protein	**Ratio of FC induction aged/young**	**P value**	**protein**	**Ratio of FC induction aged/young**	**P value**
Mrpl53	0.18	0.0077	Timm8a1	2.82	0.0404
Atxn2	0.29	0.0003	Mrps7	2.40	0.0097
Gbf1	0.30	0.0036	Nnt	2.13	0.0460
Nudt2	0.34	0.0262	Sptlc2	1.73	0.1409
Mrpl21	0.34	0.0036	Dguok	1.72	0.0918
Mrps14	0.40	0.0178	Bak1	1.71	0.0915
Uqcc2	0.46	0.0477	Mrpl2	1.58	0.0033
Ung	0.46	0.0428	Tmem126a	1.54	0.0051
Bcat1	0.46	0.0074	Slc25a22	1.54	0.0363
Pts	0.47	0.0019	Timm21	1.44	0.1639
Fpgs	0.48	0.0057	Rmdn3	1.42	0.0304
Slc16a1	0.48	0.0126	Cox7a2	1.40	0.0122
Sco2	0.52	0.0156	Eci2	1.35	0.0581
Secisbp2	0.55	0.0729	Mrpl9	1.34	0.0023
Fth1	0.56	0.0011	Ndufs6	1.33	0.3401
Dhodh	0.57	0.0239	Mthfs	1.31	0.1116
Rexo2	0.59	0.0133	Hsdl1	1.31	0.4330
Atpaf1	0.59	0.0091	Pptc7	1.30	0.0377
Mrps9	0.61	0.0068	Nudt9	1.26	0.2379
Rnmtl1	0.61	0.0809	Ndufb7	1.26	0.0037

Supplementary Figure 1, related to figures 1, 2

(**A**) Splenocytes from young and aged mice were harvested, stained, and analyzed by flow cytometry to quantify age related changes in T cell populations. Naïve CD4+ T cells were isolated from the spleen of young and aged mice, activated ex-vivo using plate-bound anti CD3/anti-CD28. Cells were harvested at 24 hrs post activation for analysis. (**B**) quantitation of early activation markers CD69 and CD25 on aged T cells, normalized to young T cells. (**C-D**) Cell were imaged by electron microscopy, and mitochondrial area was analyzed. (**C**) Size distribution of total mitochondrial population, comparing mitochondria from young and aged T cells. (**B**) Average mitochondrial size per cell.

Supplementary Figure 2, related to Figure 2.

Naïve CD4+ T cells were isolated from the spleen of young and aged mice, activated ex-vivo using plate-bound anti CD3/anti-CD28. Cells were harvested at24 hrs post activation for analysis of intracellular metabolites. Heat map summarizes the levels of single metabolites in activated aged and young $CD4^+$ T cells, calculated as the fold-change compared to average levels in young T cells.

Supplementary Figure 3, related to Figure 3.

Analysis of whole cell proteome comparing young and aged T cells (As described in Figure 3). (**A**) Log2 ratio of fold-change induction (activated/naïve) in whole cell proteome in aged vs. young T cells. Highlighted are proteins with at least 2 folds difference in induction rate between young and aged T cells. Proteins that were induced more in aged cells are shown in yellow and proteins that were induced less

in the aged cells shown in orange. (**B**) Clusters 4-12 of proteins that share similar expression kinetics during T cell activation (see Figure 3E for clusters 1-3). Proteins were clustered based on magnitude and kinetics of expression in young T cells (blue). The expression of the same cluster of proteins in aged T cells is shown in red.

Supplementary Figure 4, related to Figure 4.

Comparing mitochondrial proteome in young and aged T cells (As described in Figure 4). (**A**) Proteome data was validated by qPCR. Graph summarizes gene expression analysis of representative genes in mitochondrial one-carbon metabolism and TCA cycle.

Supplementary Figure 5, related to Figure 5.

Naïve $CD4^+$ T cells were isolated from young and aged mice, as described in Figure 1B, and activated with plate-bound anti-CD3/anti-CD28 in different concentrations: 1 μg/mL each (weak stimulation) and 4 μg/mL each (strong stimulation). Culture media was supplemented with formate + glycine, or no metabolites (control cells). Cells were harvested at 48 hr post-activation and analyzed by flow cytometry. (**A**) Representative FACS plots showing cell growth (assessed by forward scatter, FSC) under weak stimulation. (**B**) expression of the early activation marker, CD69 under weak stimulation. (**C**) expression of the early activation marker, CD69 under strong stimulation. To assess proliferation, cells were loaded with CellTrace Violet (CTV), and analyzed by flow cytometry at 48 hr post-activation. Cell divisions were detected by dilution of the CTV. (**D**) representative FACS plots showing dilution of CellTrace

Violet staining of young and aged T cells under weak stimulation. *p<0.05, ***P<0.001 (Student's t-test).

Table S1, related to figure 4.

Summary of most differentially induced proteins in the mitochondria of young and aged T cells.

Dataset S1, related to Figure 3.

Quantitation of kinetic changes in total cell proteome of young and aged $CD4^+$ T cells during the first 24 hr post activation. n=2 pools of naïve $CD4^+$ T cells (9 mice per group for aged samples and 3 mice per group for young samples) that were activated in-vitro using plate bound anti-CD3/anti-CD28, and harvested at 0, 4, and 24 hr post-activation for analysis of protein content by LC-MS^3.

Dataset S2, related to Figure 3.

Summary of most differentially induced proteins in young and aged T cells. Ration of fold change induction was calculated by dividing 24hr vs. naïve fold change induction in aged T cells by the fold change in young. Log2 values are presented.

Supplementary Experimental Procedures

Culture and stimulation of naïve CD4$^+$ T cells

Naive CD4$^+$CD62L^{hi}CD44^{lo}CD25$^-$ cells were sorted by flow cytometry (purity >99%), cultured at 37°C and 5% CO_2 in complete RPMI media (containing 10% FBS, 10mM Hepes, penicillin/streptomycin, 0.035% beta mercaptoethanol) and activated ex vivo with 4 μg/mL plate-bound anti-CD3 (clone 1H5-2C11; BioXCell) and anti-CD28 (clone 37.51; BioXCell). When indicated, different concentrations of the stimulating antibodies were used. In some experiments, formate (1mM; Sigma) glycine (400μM; Sigma), and/or folate (10mg/L; Sigma) were added to culture media at time=0, upon activation.

Flow Cytometry

Cultured cells were collected and resuspended in staining buffer (PBS with 1% FBS and 2 mM EDTA). For intracellular staining, the FoxP3 fix/perm kit (eBioscience) was used. Cell surface markers used: PE/Cy7 anti-mouse CD3 (clone 17A2), Percp/Cy5.5 anti-mouse CD4 (clone GK1.5), PE anti-mouse CD62L (clone MEL-14), APC anti-mouse CD44 (clone IM7), BV510 anti-mouse CD69 (clone H1.2F3) and BV421 anti-mouse CD25 (clone PC61) all from Biolegend. Intracellular markers: FITC anti-mouse foxp3 (clone FJK-16s, eBioscience). Cell viability was assessed using 7-AAD (Biolegend).

Electron Microscopy: sample preparation, data collection and analysis

T cells were fixed with 0.1 M cacodylate buffer, pH 7.4, containing 2% glutaraldehyde, 2% paraformaldehyde, and mixed with 4% low melting-point agarose. Imaging was done using a 1400 Transmission Electron Microscope (JEOL) equipped with a side

mount Gatan Orius SC1000 digital camera at a magnification of 20K (naïve, 4 and 9 hr) or 12K (24 hr). Micrographs were analyzed using Volocity 3D image analysis software (PerkinElmer).

Real-time PCR

Total mRNA was isolated using RNAeasy kit (Qiagen). cDNA was synthesized using the iSCRIPT kit (BioRad). Quantitative PCR analysis was performed with SYBR green, using a LightCycler 480 (Roche). *Actb*: F: 5'- AGCCATGTACGTAGCCATCC -3', R: 5'- CTCTCAGCTGTGGTGGTGAA-3'; *Shmt2*: F: 5'- GTTACCACCACCACTCACAA -3', R: 5'-TTGATTCGGTCCTCAAAGGTATAA-3'; *Mthfd1*: F: 5'-GCCATCACTGCCGCTAATA-3', R: 5'-GTCGATTGTAGAGAGCCTTGTC-3'; *Fpgs*: F: 5'-GAACGGATCCTGCGGAATTA-3', R: 5'- GGTTATAGAGGCACCAGAAGTG-3'; Aco2: F: 5'-CTCTGGACATCAGAGTAGGTTTG-3', R: 5'-TGATGGTGAACTGGGACTTG-3'; *Idh3b*: F: 5'-AGTTGCTGAACTGTACCCTAAA-3', R: 5'-GCATCACGAGCACATCAAAC-3'; *Sucla2*: F: 5'-GGAAGACGAAAGGGACAAAGA-3', R: 5'-AGCCAGCACCATTTACTAGAC-3'.

Mitochondrial respiration and glycolysis

Oxygen consumption rates and extracellular acidification rates were measured in naïve T cells isolated from young and aged male C57Bl/6 mice. Measurements were done in non-buffered DMEM containing 5 mM glucose, 2 mM L-glutamine, and 1 mM sodium pyruvate, under basal conditions and in response to mitochondrial inhibitors: 5 μM oligomycin, 1 μM FCCP, 100 nM rotenone, and 1 μM antimycin A (All from Sigma) using the XF24 Extracellular Flux Analyzer (Seahorse Bioscience).

Metabolomics

For analysis of metabolite content by mass spectrometry, activated $CD4^+$ T cells were collected into eppendorf tubes, centrifuged at 10,000 rpm for 30 sec at room temperature, resuspended in 1 mL HBSS, and promptly centrifuged again under the same conditions. The supernatant was quickly removed, and the pellets extracted with 50µl extraction buffer (40% acetonitrile/40% methanol/20% water + 0.5% formic acid). Total time from perturbation of the cells to quenching was ~ 1 min. Samples were incubated 5-10 min on ice followed by pH neutralization with 15% w/v ammonium hydroxide. Samples were stored at -80°C, followed by centrifugation at 4°C (~15,000 rcf) to remove insoluble cell components. The supernatants were analyzed using a quadrupole-orbitrap mass spectrometer (Q Exactive Plus, Thermo Fisher Scientific, Waltham, MA) coupled to liquid chromatography (LC) methods via electrospray ionization. LC separation for monitoring metabolites in negative-ion mode was achieved using hydrophilic interaction chromatography on a XBridge BEH Amide column (2.1 mm x 150 mm, 2.5 µm particle size, 130 Å pore size; Waters, Milford, MA) using a gradient of solvent A (20 mM ammonium acetate + 20mM ammonium hydroxide in 95:5 water:acetonitrile, pH 9.45) and solvent B (acetonitrile). LC separation for monitoring metabolites in positive-ion mode was achieved using reverse-phase chromatography on an InfinityLab Poroshell 120 (2.1 mm x 150 mm, 2.7 µm particle size, 120 Å) using a gradient of solvent A (10 mM ammonium acetate + 0.1% acetic acid in 98:2 water:acetonitrile, pH 3) and solvent B (acetonitrile).

Proteomics sample preparation and data analysis

Cell lysis and protein digestion

Cells were homogenized by 10 passes through a 21-gauge (1.25 inches long) needle. The homogenate was sedimented by centrifugation at 21,000 x *g* for 5 min and the supernatant was transferred to a new tube. Protein concentrations were determined using the bicinchoninic acid (BCA) assay (ThermoFisher Scientific). Proteins were subjected to disulfide bond reduction with 5 mM tris (2-carboxyethyl)phosphine (room temperature, 30 min) and alkylation with 10 mM iodoacetamide (room temperature, 30 min in the dark). Excess iodoacetamide was quenched with 10 mM dithiotreitol (room temperature, 15 min in the dark). Trichloroacetic acid precipitation was performed prior to protease digestion. In brief, 100% TCA was added to each designated sample to achieve a final concentration of 12.5%. The sample was vortexed, incubated on ice for 1 hr, and centrifuged at 20,000 RPM for 30 min at 4^0C. The supernatant was aspirated and the sample was washed once with 0.5 mL of acetone. The sample was centrifuged at 20,000 RPM for 10 min at 4^0C. The supernatant was aspirated and the sample was washed once with 0.5 mL of methanol and allowed to air-dry. Samples were resuspended in 200 mM EPPS, pH 8.5 by sonication, and digested at room temperature for 13 h with Lys-C protease at a 100:1 protein-to-protease ratio. Trypsin was then added at a 100:1 protein-to-protease ratio and the reaction was incubated for 6 h at 37°C.

Tandem mass tag labeling

30% acetonitrile (v/v) was added to samples containing ~20 µg of peptides, with 2 µL of TMT reagent (20 ng/µL). Following incubation at room temperature for 1.5 hrs, the reaction was quenched with hydroxylamine to a final concentration of 0.3% (v/v)

for 15 min. The TMT-labeled samples were pooled based on cell numbers, and the combined sample was vacuum centrifuged to near dryness and subjected to C18 solid-phase extraction (SPE) via Sep-Pak (Waters, Milford, MA).

Off-line basic pH reversed-phase (BPRP) fractionation

Pooled TMT-labeled peptide sample was fractionated using the Pierce High pH Reversed-Phase Peptide Fractionation Kit. 12 fractions were collected using: an acetonitrile gradient. From here, every 6th sample was combined, yielding a total of 6 samples. Samples were subsequently acidified with 1% formic acid and vacuum centrifuged to near dryness. Each fraction was desalted via StageTip, dried again via vacuum centrifugation, and reconstituted in 5% acetonitrile, 5% formic acid for LC-MS/MS processing.

Liquid chromatography and tandem mass spectrometry

Mass spectrometry data were collected using an Orbitrap Fusion Lumos mass spectrometer (Thermo-Fisher Scientific, San Jose, CA) coupled to a Proxeon EASY-nLC 1200 liquid chromatography (LC) pump (ThermoFisher Scientific, San Jose, CA). Peptides were separated on a 100 μm inner diameter microcapillary column packed with ~40 cm of Accucore150 resin (2.6 μm, 150 Å, ThermoFisher Scientific, San Jose, CA). For each analysis, we loaded ~2 μg onto the column and separation was achieved using a 2.5 h gradient of 7 to 27% acetonitrile in 0.125% formic acid at a flow rate of ~550 nL/min. Each analysis used an SPS-MS3-based TMT method (1, 2), which has been shown to reduce ion interference compared to MS2 quantification (3). The scan sequence began with an MS1 spectrum (Orbitrap; resolution 120,000; mass range

400–1400 m/z; automatic gain control (AGC) target 5×10^5; maximum injection time 100 ms). Precursors for MS2/MS3 analysis were selected using a Top10 method. MS2 analysis consisted of collision-induced dissociation (quadrupole ion trap; AGC 1.8×10^4; normalized collision energy (NCE) 35; maximum injection time 150 ms). Following acquisition of each MS2 spectrum, we collected an MS3 spectrum using our recently described method in which multiple MS2 fragment ions were captured in the MS3 precursor population using isolation waveforms with multiple frequency notches (2). MS3 precursors were fragmented by high energy collision-induced dissociation (HCD) and analyzed using the Orbitrap (NCE 55; isolation window 1.2 Th, AGC 3×10^5; maximum injection time 120 ms, resolution was 50,000 at 200 Th).

Data extraction and protein quantification

Mass spectra were processed using a Sequest-based in-house software pipeline (4). Spectra were converted to mzXML using a modified version of ReAdW.exe. Database searching included all entries from the mouse UniProt database (April 20, 2016). This database was concatenated with one composed of all protein sequences in the reversed order. Searches were performed using a 50 ppm precursor ion tolerance for total protein level profiling. The product ion tolerance was set to 0.9 Da. These wide mass tolerance windows were chosen to maximize sensitivity in conjunction with Sequest searches and linear discriminant analysis (4, 5). TMT tags on lysine residues and peptide N termini (+229.163 Da) and carbamidomethylation of cysteine residues (+57.021 Da) were set as static modifications, while oxidation of methionine residues (+15.995 Da) was set as a variable modification. Peptide-spectrum matches (PSMs)

were adjusted to a 1% false discovery rate (FDR) (6, 7). PSM filtering was performed using a linear discriminant analysis, as described previously (4), while considering the following parameters: XCorr, ΔCn, missed cleavages, peptide length, charge state, and precursor mass accuracy. For TMT-based reporter ion quantitation, we extracted the summed signal-to-noise (S/N) ratio for each TMT channel and found the closest matching centroid to the expected mass of the TMT reporter ion. PSMs were identified, quantified, and collapsed to a 1% peptide false discovery rate (FDR) and then collapsed further to a final protein-level FDR of 1%. Moreover, protein assembly was guided by principles of parsimony to produce the smallest set of proteins necessary to account for all observed peptides. Proteins were quantified by summing reporter ion counts across all matching PSMs using in-house software, as described previously (4). PSMs with poor quality, MS3 spectra with more than eight TMT reporter ion channels missing, MS3 spectra with TMT reporter summed signal-to-noise ratio less than 100, or no MS3 spectra were excluded from quantification (8).

1. Ting, L.; Rad, R.; Gygi, S. P.; Haas, W., MS3 eliminates ratio distortion in isobaric multiplexed quantitative proteomics. *Nat Methods* **2011,** 8, (11), 937-40.

2. McAlister, G. C.; Nusinow, D. P.; Jedrychowski, M. P.; Wuhr, M.; Huttlin, E. L.; Erickson, B. K.; Rad, R.; Haas, W.; Gygi, S. P., MultiNotch MS3 enables accurate, sensitive, and multiplexed detection of differential expression across cancer cell line proteomes. *Anal Chem* **2014,** 86, (14), 7150-8.

3. Paulo, J. A.; O'Connell, J. D.; Gygi, S. P., A Triple Knockout (TKO) Proteomics Standard for Diagnosing Ion Interference in Isobaric Labeling Experiments. *J Am Soc Mass Spectrom* **2016,** 27, (10), 1620-5.

4. Huttlin, E. L.; Jedrychowski, M. P.; Elias, J. E.; Goswami, T.; Rad, R.; Beausoleil, S. A.; Villen, J.; Haas, W.; Sowa, M. E.; Gygi, S. P., A tissue-specific atlas of mouse protein phosphorylation and expression. *Cell* **2010,** 143, (7), 1174-89.

5. Beausoleil, S. A.; Villen, J.; Gerber, S. A.; Rush, J.; Gygi, S. P., A probability-based approach for high-throughput protein phosphorylation analysis and site localization. *Nat Biotechnol* **2006,** 24, (10), 1285-92.

6. Elias, J. E.; Gygi, S. P., Target-decoy search strategy for mass spectrometry-based proteomics. *Methods Mol Biol* **2010,** 604, 55-71.

7. Elias, J. E.; Gygi, S. P., Target-decoy search strategy for increased confidence in large-scale protein identifications by mass spectrometry. *Nat Methods* **2007,** 4, (3), 207-14.

8. McAlister, G. C.; Huttlin, E. L.; Haas, W.; Ting, L.; Jedrychowski, M. P.; Rogers, J. C.; Kuhn, K.; Pike, I.; Grothe, R. A.; Blethrow, J. D.; Gygi, S. P., Increasing the multiplexing capacity of TMTs using reporter ion isotopologues with isobaric masses. *Anal Chem* **2012,** 84, (17), 7469-78.